To appear in:
Phys. Lett. A

A quantum cable car for Wannier-Stark ladders

M. Glück, A. R. Kolovsky[*] and H. J. Korsch

Fachbereich Physik, Universität Kaiserslautern, D-67653 Kaiserslautern, Germany

September 29, 2000

Abstract. The paper studies the dynamics of transitions between the levels of a Wannier-Stark ladder induced by a resonant periodic driving. The analysis of the problem is done in terms of resonance quasienergy states, which take into account the metastable character of the Wannier-Stark states. It is shown that the periodic driving creates from a localized Wannier-Stark state an extended Bloch-like state with a spatial length varying in time as $\sim t^{1/2}$. Such a state can find applications in the field of atomic optics because it generates a coherent pulsed atomic beam.

PACS. 7 3.20Dx, 03.65.-w; 42.50.Vk ; Keywords: Wannier-Stark ladder; induced transitions

1 Introduction

The term Wannier-Stark ladder (WSL) is currently used in the literature to denote a set of equally spaced levels

$$E_{\alpha,l} = E_\alpha + aFl\ , \quad l = 0, \pm 1, \dots\ , \quad \alpha = 0, 1, \dots\ , \quad (1)$$

of a Bloch particle in a homogeneous field:

$$\widehat{H}_W = \widehat{H}_0 + Fx\ , \quad (2)$$

$$\widehat{H}_0 = \hat{p}^2/2m + V(x)\ , \quad V(x+a) = V(x)\ ,$$

(a model of a crystal electron subject to a static electric field). In this paper we study the dynamics of the transitions between the Wannier levels induced by a resonant periodic driving

$$\widehat{H} = \widehat{H}_W - F_\omega x \cos(\omega t)\ , \quad \hbar\omega = aF\ . \quad (3)$$

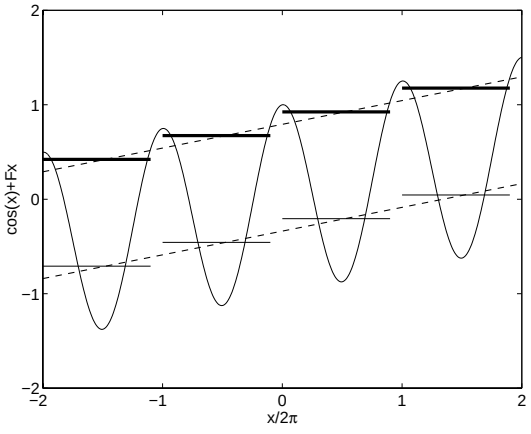

Fig. 1. WSL for a cosine potential. The dashed lines indicate the transitions induced by the resonant periodic driving.

As illustrated in Fig. 1, the resonant driving couples the levels belonging to the same WSL, but the transitions to the exited WSL are strongly detuned and can be neglected. Then, assuming that initially only one level is occupied, it shifts the probability up and down the ladder, acting as a 'cable car'. The analysis of this process is the central aim of the present work. We have found that the distribution function for the occupation probability evolves in a highly nontrivial way and has different short- and long-time regimes. This is shown to be due to the fact that the Wannier-Stark states (WS-states) are actually metastable states and, therefore, the WSL levels have a finite width.

The structure of the paper is as follows. Section 2 analyzes a simplified problem, where the WS-states are assumed to be stationary energy states. The effect of the finite life-time of the WS-states (i.e. a finite level width) is discussed in Sec. 3. Section 4 compares the analytical results of Sec. 2 and Sec. 3 with a direct numerical simulation of the quantum dynamics of system (3). Finally, in Sec. 5, we discuss a possible application of the results obtained in relation to the experiments with cold atoms in an optical lattice [1].

In what follows we restrict ourselves to the case of the ground WSL [then we shall omit the index α in Eq. (1)] and, to be concrete, we choose the periodic potential in the form $V(x) = V_0 \cos(2\pi x/a)$. Moreover, to simplify the formula, we choose units with $m = 1$, $V_0 = 1$, and $a = 2\pi$. Then the independent parameters of the system (3) are the amplitude of the static force, F, the amplitude of the driving force, F_ω, and the scaled Planck constant $\hbar$ entering the momentum operator [3]. The value of the driving frequency ω is fixed by the condition $\hbar\omega = 2\pi F$.

2 Tight-binding model

The simplest approach to the problem uses the tight-binding model. In the frame of this model the system (2) is approximated by the Hamiltonian

$$H_W = H_0 + F\sum_l |l\rangle 2\pi l \langle l| \,, \tag{4}$$

$$H_0 = E\sum_l |l\rangle\langle l| + \frac{\Delta}{2}\sum_l \left(|l\rangle\langle l+1| + |l+1\rangle\langle l|\right) \,,$$

where $|l\rangle$ denotes the localized Wannier state associated with the l-th site of the lattice. The eigenstates of the Hamiltonian H_0 are the Bloch waves $|\phi_k\rangle = \sum_l e^{i2\pi lk}|l\rangle$ corresponding to the energy $E(k) = E + \Delta\cos(2\pi k)$. Referring to the system (2) with $V(x) = \cos x$ this dispersion relation is a good approximation of the ground Bloch band for $\hbar \le 2$. Correspondingly, the minimal uncertainty wave packet (coherent state)

$$\Phi_l(x) = (\pi\hbar)^{-1/4}\exp\left[-(x-x_l)^2/2\hbar\right] \tag{5}$$

located at $x = \pi(2l+1)$ is a good approximation for the localized state $|l\rangle$. The eigenstates of the Hamiltonian H_W are known to be

$$|\Psi_l\rangle = \sum_m J_{m-l}\left(\frac{\Delta}{2\pi F}\right)|m\rangle \,, \tag{6}$$

(here $J_m(z)$ is the ordinary Bessel function) and correspond to the energies $E_l = E + 2\pi Fl$. For the sake of simplicity we restrict ourselves to the case

$$2\pi F \gg \Delta \,. \tag{7}$$

Then the WS-states (6) approximately coincide with the localized state $|l\rangle$.

We proceed with the case of a resonant periodic driving

$$H = H_0 + [F - F_\omega\cos(\omega t)]\sum_l |l\rangle 2\pi l\langle l| \tag{8}$$

with $\hbar\omega = 2\pi F$. Provided the condition (7) is satisfied, the quasienergy states (i.e. the eigenfunctions of the evolution operator over the period of the driving force) can be approximated by Bloch waves with time-dependent quasi-momentum $k(t) = k - Ft/\hbar + (F_\omega/\hbar\omega)\sin(\omega t)$. The corresponding quasienergies form a band

$$E(k) = E + J_1\left(\frac{F_\omega}{F}\right)\Delta\cos(2\pi k) \,, \tag{9}$$

which recovers the original Bloch dispersion relation, however, with a renormalized width [2].

It is convenient to measure the time in units of the driving (Bloch) period $T_B = \hbar/F = 2\pi/\omega$ (we shall denote this discrete time by τ in what follows). Then the general solution of the Schrödinger equation can be presented in the form

$$|\psi(\tau)\rangle = \int_{-1/2}^{1/2} \mathrm{d}k\, a(k)\, e^{-i2\pi E(k)\tau/\hbar\omega}|\Psi_k\rangle \equiv \sum_l c_l(\tau)|l\rangle \,, \tag{10}$$

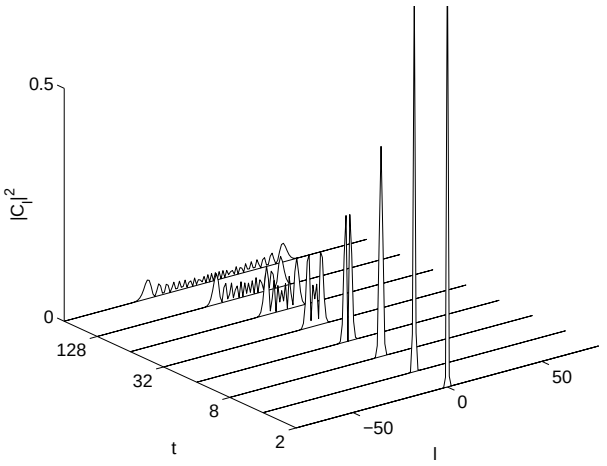

Fig. 2. Occupation probability of the WSL levels as a function of time in the tight-binding approximation. The plot is generated on the basis of Eq. (11) for $z = -0.15$.

where $|\Psi_k\rangle \approx \sum_l e^{i2\pi lk}$ are the quasienergy Wannier-Bloch states (WB-states) and the function $a(k)$ is specified by the initial condition. In particular, when only one WSL level is populated at $t = 0$ (let it be $l = 0$), the probability amplitudes $c_l(\tau)$ are given (up to the irrelevant phase factor) by the ordinary Bessel functions

$$c_l(\tau) = (-i)^l J_l(z\tau) \,, \quad z = \frac{2\pi\Delta}{\hbar\omega}J_1\left(\frac{F_\omega}{F}\right) \,. \tag{11}$$

As an example, Fig. 2 shows the occupation probability calculated on the basis of Eq. (11) for $z = -0.15$. It is seen that the number of populated levels grows linearly with time. However, as shown in the next section, Eq. (11) has only limited validity and gives a wrong result for large τ.

3 Decay of the WS-states

The main drawback of the tight-binding approach used in Sec. 2 is that it entirely neglects the decay of the WS-states, which is due to the tunneling and can be characterized by the width Γ of the levels: $\mathcal{E}_l = E_l - i\Gamma/2$.

In what follows it will be useful to analyze the system dynamics in phase-space, e.g. by using the Husimi representation of the wave function. For a given wave function $\psi(x)$ the Husimi function is defined as $h(p,q) = |\langle p,q|\psi\rangle|^2$, where $\langle x|p,q\rangle = (\pi\hbar)^{-1/4}\exp[-(x-q)^2/2\hbar + ipx]$ is a coherent state. Alternatively, the Husimi function can be obtained by smoothing the Wigner function. Similar to the Wigner function, the Husimi function joins the coordinate and momentum representations. However, unlike the Wigner function, it is nonnegative, which allows the direct comparison of quantum dynamics with classical dynamics in phase space.

Figure 3 shows the ground metastable WS-state (or Wannier-Stark resonance) for $\hbar = 2$, $F = 0.08$, and $l = 0$

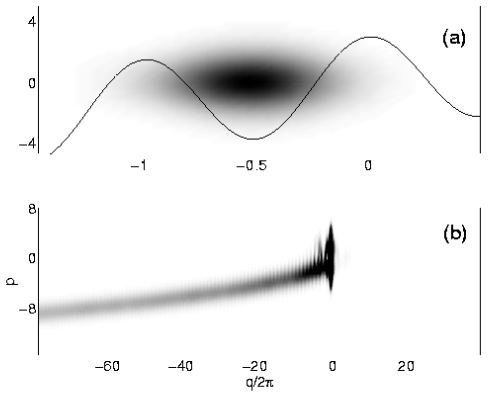

Fig. 3. Ground WS-state for $\hbar = 2$, $F = 0.08$, and $l = 0$ in the Husimi phase-space representation. Taking the upper limit of the grey-scale axis for the upper plot (a) to be unity, it is reduced 800 times in the lower plot (b) to make the probability flow visible.

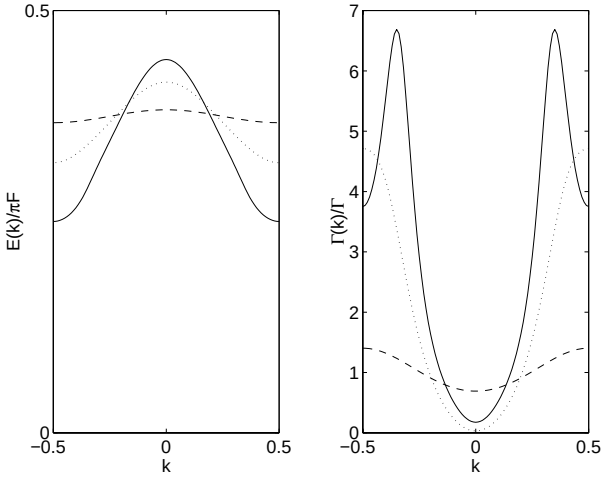

Fig. 4. Real (left panel) and imaginary (right panel) parts of the ground quasienergy band of the system (3) for $\hbar = 2$, $F = 0.08$, and $F_\omega = 0.0032$ (dashed line), $F_\omega = 0.0189$ (dotted line), $F_\omega = 0.0379$ (solid line). The width of the unperturbed Wannier-Stark resonance is $\Gamma = 0.0140F$.

in the Husimi representation. (We note that for $\hbar = 2$ the width of the ground Bloch band is $\Delta = 0.17$ and, thus, condition (7) is satisfied.) A comet-like structure is seen where the head of the comet approximately corresponds to the Husimi image of the localized state (5). The tail of the comet is the quantum probability tunneling out of the potential well. The shape of this tail is parabolic because of the acceleration of the particle according to the classical equations $p(t) = -Ft$ and $x(t) = -Ft^2/2$. The width of the displayed resonance state is $\Gamma = 0.0140F$, which corresponds to the decay time $\hbar/\Gamma = 71T_B$, $T_B = \hbar/F$. For the definition and properties of the WS-states, for example, the dependence of the lifetime on F, we refer to the recent papers [3,4]. Here we only note that the WS-states are resonance eigenfunctions of the Hamiltonian (2) and, therefore, one should distinguish between the left, $\Psi_l^{(L)}(x)$, and the right, $\Psi_l^{(R)}(x)$, eigenfunctions. (Then the orthogonality relation $\langle l|l'\rangle = \delta_{l,l'}$ reads as $\int \mathrm{d}x \Psi_l^{(L)}(x)\Psi_{l'}^{(R)}(x) = \delta_{l,l'}$.)

Because the energies of the WSL levels are complex, the quasienergy spectrum is also expected to be complex. For the resonant case $\hbar\omega = 2\pi F$ considered here the complex quasienergy spectrum $\mathcal{E}(k) = E(k) - i\Gamma(k)/2$ of the system (3) is analyzed in Ref. [4]. In first order of F_ω the dispersion relation for the quasienergy $\mathcal{E}$ has the form

$$E(k) = E + \frac{F_\omega}{F}\mathrm{Re}\Delta\cos(2\pi k)\ , \qquad (12)$$

$$\Gamma(k) = \Gamma + \frac{F_\omega}{F}\mathrm{Im}\Delta\cos(2\pi k)\ . \qquad (13)$$

In Eq. (12) $\mathrm{Re}\Delta$ coincides with the Bloch band width and we introduce the notion of $\mathrm{Im}\Delta \sim \Gamma$ in Eq. (13) to take into account the finite band width for the imaginary part of the quasienergy spectrum. We would like to stress that the displayed equations are valid only under the condition $F_\omega \ll F$. For larger amplitudes of the driving force there is a deviation from the cosine dependence for $\mathcal{E}(k)$ (see Fig. 4). In particular, as the imaginary part is concerned, there is some critical value of $F_\omega^c \sim F$ when the decay rate of the quasienergy WB-states corresponding to the center of the Brillouin zone decreases almost to zero [5]. For F_ω close to F_ω^c (but $F_\omega < F_\omega^c$) the equation $\Gamma(k) = \Gamma[1 + (F_\omega/F_\omega^c)\cos(2\pi k)]^2$ is a better approximation to $\Gamma(k)$ than Eq. (13). The pronounced dependence of the imaginary part of the quasienergy spectrum on the quasimomentum leads to markedly different decay times of the corresponding quasienergy states, i.e. a selective decay of the quasienergy WB-states.

In Sec. 2 we derived the equation defining the population of the WSL levels in the tight-binding approximation [see Eq. (11)]. This equation was obtained by neglecting the decay of the quasienergy WB-states. Obviously, in order to include this effect, Eq. (11) should be modified as

$$c_l(\tau) = \exp\left(-\frac{\pi\Gamma}{\hbar\omega}\tau\right)(-i)^l J_l(z\tau)\ , \qquad (14)$$

$$z = (\mathrm{Re}\Delta - i\mathrm{Im}\Delta)\frac{2\pi F_\omega}{\hbar\omega F}\ .$$

where the exponential prefactor in Eq. (14) accounts for the overall decay of the probability. The complex correction to the argument of the Bessel function is responsible for the selective decay of the quasienergy states. Figure 5 shows the population of the WSL levels calculated for a complex value $z = -0.15 + i0.011$. By comparing Fig. 5 with Fig. 2 one concludes that the short-time regime of the transition dynamics is described by the dispersion process in accordance with Eq. (11). However, after a characteristic time $\tau^c \approx 1/\mathrm{Im}(z)$ the process of selective decay

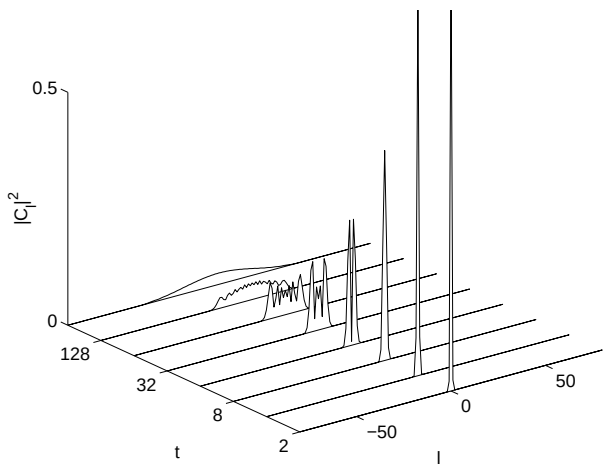

Fig. 5. Occupation probability of the WSL levels as a function of time. The plot is generated on the basis of Eq. (14) for $z = -0.15 + i0.011$. To compensate the effect of overall decay the coefficients $c_l(\tau)$ are renormalized at each time.

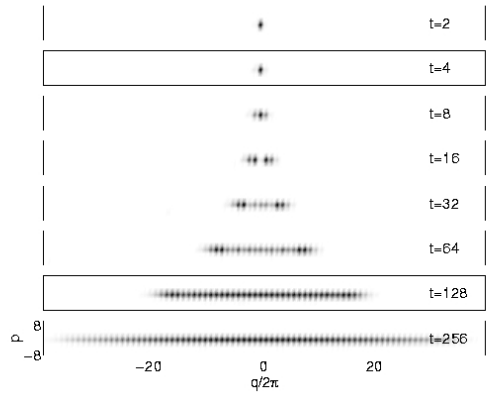

Fig. 6. Time evolution of the coherent state (5) in the Husimi representation. Parameters are $\hbar = 2$, $F = 0.08$, and $F_\omega = 0.0189$.

dominates the dispersion and the probability distribution becomes close to the Gaussian distribution

$$|c_l(\tau)| \sim \exp\left(-\frac{2\pi^2|\mathrm{Im}z|l^2}{\tau|z|^2}\right) . \qquad (15)$$

We note that according to Eq. (15) the number of populated levels grows now as $\sim t^{1/2}$.

4 Wave packet dynamics

To check the theoretical predictions of Sec. 3 we simulated the wave packet dynamics of the system (3) for $\hbar = 2$, $F = 0.08$ and $F_\omega = 0.3/\omega^2 \approx 0.019$. As an initial condition we choose a minimal uncertainty wave packet (5) located in the well with $l = 0$.

Figure 6 shows the evolution of the initial wave packet in the Husimi representation. It is seen that at any time the wave function is a superposition of the states localized in the wells of the cosine potential. Thus we can introduce the notion of the probability amplitude for the l-th potential well

$$c_l(\tau) = \int \mathrm{d}x \Phi_l^*(x)\psi(x,\tau) , \qquad (16)$$

where $\Phi_l(x)$ is given by Eq. (5) [6]. The corresponding occupation probabilities $|c_l(\tau)|^2$ are shown in Fig. 7. This figure should be compared with Fig. 5 in which the value of z was chosen such as to obtain a possibly best approximation to the exact dispersion relation $\mathcal{E}(k)$ (dotted line in Fig. 4) by a cosine function. A reasonable correspondence is noticed.

In the rest of this section we discuss the coherence properties of the wave packet $\psi(x,t)$. An important characteristic of $\psi(x,t)$ is the coherence length δL which we introduce as a characteristic length for the decay of the correlation function

$$R_\tau(L) = P^{-1}(\tau)\sum_l c_l^*(\tau)c_{l+L}(\tau) , \qquad (17)$$

where the $c_l(\tau)$ are given in Eq. (16) and $P(\tau) = \sum_l |c_l(\tau)|^2$ is the total probability.

First we discuss the behavior of the correlation function (17) within the frame of the modified tight-binding model. Substituting Eq. (14) into Eq. (17) and using the summation rule for the Bessel functions (Graf's generalization of the Neumann formula) we obtain

$$R_\tau(L) = (-i)^L J_L(i2|\mathrm{Im}z|\tau) . \qquad (18)$$

It follows from Eq. (18) that the coherence length grows as $\delta L \sim (|\mathrm{Im}z|\tau)^{1/2}$. We would like to stress that this result is solely due to the nonunitary evolution. In the case of

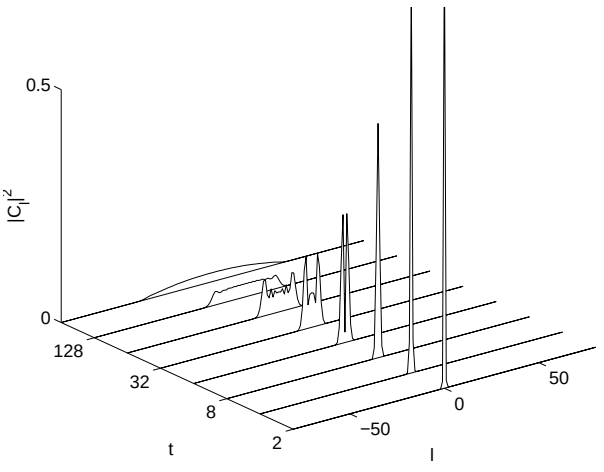

Fig. 7. Occupation probabilities of the WSL levels for the case shown in Fig. 6. Similar to Fig. 5, the occupation probabilities are renormalized at each time.

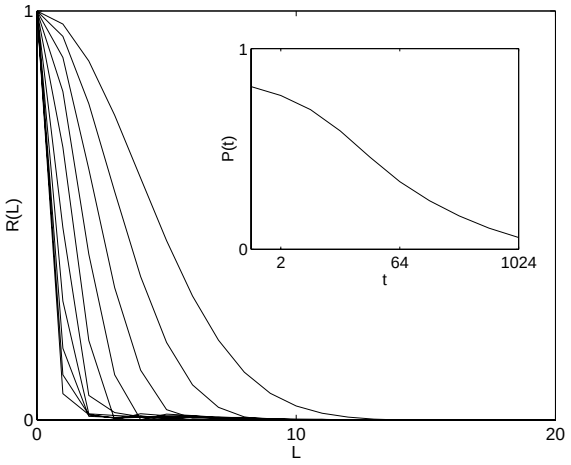

Fig. 8. Correlation function (17) for $\tau = 2, 4, \ldots, 1024$ calculated numerically on the basis of the wave packet dynamics of system (3). The inset shows the decay of the total probability $P(\tau)$.

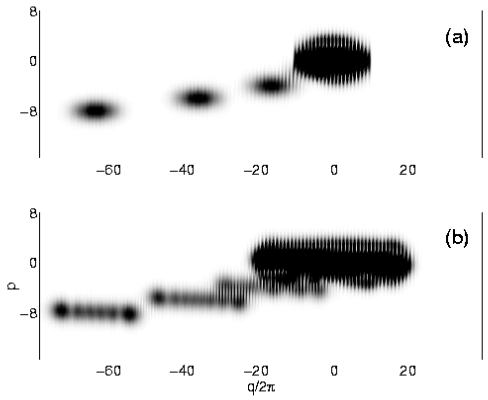

Fig. 9. (a) Observation of the Bloch oscillations in the case of a coherent initial condition (21). The Husimi phase-space representation of $\psi(x,t)$ for $t = 128T_B$ is shown. (b) The same as in case (a) but for an initial condition in the form of a wave packet prepared from the localized state $\Phi_0(x)$ by periodic resonant driving of the system for 128 periods (see Fig. 6.)

the celebrated tight-binding model (unitary evolution, see Sec. 2) the coherence length is zero for arbitrary times.

To check the estimate (18) we calculated numerically the function $R_\tau(L)$ on the basis of wave packet dynamics (see Fig. 8). The ten curves in the figure correspond to times $\tau = 2, 4, \ldots$, up to $\tau = 1024$. A good overall agreement with the Eq. (18) is noticed.

Next we consider a quantity $S = \mathrm{Tr}\,\hat\rho^2/(\mathrm{Tr}\,\hat\rho)^2$, which is commonly used to distinguish a pure state ($S = 1$) from a statistical mixture ($S < 1$). In particular, we shall be interested in an initial condition where $\hat\rho(t = 0)$ is diagonal in the basis of the WS-states. In this case the following relation can be easily obtained

$$S(\tau) = \frac{\mathrm{Tr}\,\hat\rho^2(\tau)}{\left(\mathrm{Tr}\,\hat\rho(\tau)\right)^2} = \sum_{l,m} \rho_{l,l}\rho_{m,m} R_\tau(l-m)\ . \qquad (19)$$

It is seen from Eq. (18) and Eq. (19) that in course of the time evolution the quantity $S(\tau)$ monotonically increases and approaches unity when the coherence length δL exceeds the 'localization length' ΔL of the initial state (we implicitly assume that $\rho_{l,l} \approx 0$ for $|l| \gg \Delta L$). Thus the resonant periodic driving can be used to create a pure quantum state from the statistical mixture. In the next section we consider a possible application of this result in the field of atomic optics.

5 Bloch oscillations in an optical lattice

In this section we discuss the dynamics of the system (3) in connection with the experiment [1] where the Bloch oscillations for neutral atoms in the optical lattice were observed. In this experiment cold rubidium atoms were placed in a vertically aligned standing laser wave. (The atoms were first captured and cooled by using a MOT and then the standing laser wave was switched on adiabatically.) The laser frequency is detuned far from the resonant transition of the rubidium atom. Then the atoms are subject only to the potential force of the optical potential $V(z) = V_0 \cos^2(k_L z)$ (k_L is the laser wave vector and the amplitude V_0 is proportional to the laser intensity) and the gravitational force. The depth of the optical potential V_0 was adjusted to insure a noticeable tunneling. Thus the atoms can leak out of the potential wells producing an atomic beam.

The key point of the experiment [1] is that the atoms were prepared in the state where the atomic wave function extends over several lattice periods. Namely, at $t = 0$ the single-particle wave function $\psi(x,0)$ is believed to be

$$\psi(x,0) = \sum_l c_l \Phi_l(x)\ ,$$
$$c_l = \frac{1}{(2\pi)^{1/4}(\Delta L)^{1/2}} \exp\left(-\frac{l^2}{4(\Delta L)^2}\right)\ , \qquad (20)$$

where ΔL is the spatial size of the atomic array. According to Eq. (17), the coherence length δL of this packet coincides with ΔL. Because the atoms are neutral the interaction between them can be neglected [8] and the one-particle density matrix factorizes as $\rho(x,x') = N^{-1} \sum_{n=1}^{N} \psi^{*(n)}(x)\ \psi^{(n)}(x')$ where the sum over n denotes the sum over the atoms. In what follows we assume the $\psi^{(n)}(x)$ to be identical and given by Eq. (20). Then $\rho(x,x')$ takes the form

$$\rho(x,x') = \sum_{l,l'} c_l^* c_{l'} \Phi_l^*(x)\Phi_{l'}(x)\ . \qquad (21)$$

Because $\mathrm{Tr}\rho^2(x,x') = 1$, we shall refer to Eq. (21) as the case of completely coherent initial condition.

We simulated the dynamics of the initial state (21) numerically. It was found that, after a short transient, the initial wave packet evolves according to the equation [7]

$$\psi(x,t) = \sum_l \tilde{c}_l \exp(-i\mathcal{E}_l t/\hbar)\Psi_l^{(R)}(x) \ , \qquad (22)$$

where $\Psi_l^{(R)}(x)$ is resonance WS-state, $\mathcal{E}_l$ its complex energy and $\tilde{c}_l = \int \mathrm{d}x\, \Psi_l^{(L)}(x)\psi(x,0) \approx c_l$. The upper panel (a) in Fig. 9 shows the function (22) for $t = 128T_B$. It is seen that the atomic array emits every Bloch period a drop of atoms which then becomes accelerated by the gravitational force.

This drop-like behavior (well observed in the laboratory experiment) should be opposed to the continuous beam in the case of incoherent initial condition. In the latter case each atom occupies a single well and the one-particle density matrix has the form

$$\rho(x,x') = \sum_l |c_l|^2 \Phi_l^*(x)\Phi_l(x') \ , \qquad (23)$$

where $|c_l|^2$ is the occupation probability of the l-th well. [Similar to Eq. (21) we asume that $|c_l|^2 \sim \exp[-l^2/2(\Delta L)^2]$, where ΔL is the spatial size of the atomic array. Let us also note that the density matrix (23) can be formally obtained from density matrix (21) by assuming random phases of the expansion coefficients c_l in Eq. (20.] As seen from Eq. (23), the dynamics of the system in the case of incoherent initial condition is defined by the dynamics of the wave packet $\psi(x,0) = \Phi_l(x)$ which is $\psi(x,t) \approx \exp(-i\mathcal{E}_l t/\hbar)\Psi_l(x)$ [see Fig. 3(b)]. Since the correlation length of this packet is zero, the Bloch oscillation does not show up and the probability flow is continuous.

In conclusion, in order to observe Bloch oscillations one should create a wave packet with nonzero coherence length. In the experiment [1] this was done by using a Bose-Einstein condensate. At higher temperature, however, the required wave packet can be created by using the resonant driving. As an example, the lower panel (b) in Fig. 9 shows the atomic pulses emitted by a wave packet which was obtained from the localized state $\Phi_0(x)$ by driving the system for 128 periods. (To have a complete picture, the displayed Husimi function should be summed up with its replica shifted by l and weighted by $|c_l|^2$. However, this averaging procedure does not change the pulsed character of the emitted beam.) The duration of the pulses is obviously determined by the spatial extent of the created wave packet and can be easily varied.

6 Conclusion

We studied the dynamics of transitions between the Wannier-Stark levels induced by a resonant periodic driving. Since each level of the Wannier-Stark ladder is associated with a state essentially localized within the l-th potential well, this problem can also be formulated as a transport phenomenon. It was shown that the resonant periodic driving causes a spreading of an initially localized wave packet over the lattice. The short-time regime of spreading is linear in time and can be treated as a dispersion. However, this regime is changed into a $t^{1/2}$-spreading for large time. It is argued in the paper that this $t^{1/2}$-spreading is a consequence of the selective decay of the quasienergy Wannier-Bloch states. The other consequence of this selective decay is a pronounced increase of the coherence length of the wave packet.

As an application of this effect we considered the Bloch oscillations of neutral atoms in an optical lattice. The Bloch oscillation is a coherent phenomenon and can be observed only in the case of coherent initial conditions (21). Because the preparation of this state is a rather difficult experimental problem, we considered the case of an incoherent initial condition (23). It was shown in the paper that the coherence properties of the initial state (23) can be 'improved' by means of resonant driving, so that the Bloch oscillations become visible.

References

[*] Also at L. V. Kirensky Institute of Physics, 660036 Krasnoyarsk, Russia.

1. B. P. Anderson and M. A. Kasevich, Science **282**, (1998) 1686.
2. D. H. Dunlap and V. M. Kenkre, Phys. Rev. B **34**, (1986) 3625; Nguyen Hong Shon and H. N. Nazareno, J. Phys.: Condensed Matter **4**, (1992) L611; X.-G. Zhao, R. Jahnke, and Q. Niu, Phys. Lett. A **202**, (1995) 297; M. Holthaus, G. H. Ristov, and D. W. Hone, Europhys. Lett., **32**, (1995) 241; K. Drese and M. Holthaus, Phys. Rev. Lett. **78**, (1997) 2932.
3. M. Glück, A. R. Kolovsky, H. J. Korsch, and N. Moiseyev, EPJ D**4**, (1998) 239; M. Glück, A. R. Kolovsky, and H. J. Korsch, Phys. Rev. Lett. **82**, (1999) 1534; Phys. Rev. E **60**, (1999) 247; Phys. Rev. Lett. **83**, (1999) 891.
4. M. Glück, A. R. Kolovsky, and H. J. Korsch, Phys. Lett. A **258**, (1999) 383.
5. The position of the minimum of $\Gamma(k)$ actually depends on the difference between the phase of the Bloch oscillations and the phase of the driving force. For example, by substituting $\cos(\omega t)$ in the Hamiltonian (3) by $\cos(\omega t + \phi)$ we can shift the curves in Fig. 4 by $\Delta k = \phi/2\pi$.
6. Equation (16) assumes the approximation of the WS-states by the coherent states (5). Without this approximation Eq. (16) reads as $c_l(\tau) = \int \mathrm{d}x\, \Psi_l^{(L)}(x)\psi(x,\tau)$, where $\Psi_l^{(L)}(x)$ is the left eigenfunction.
7. Equation (22) is valid only for $|x| < x_{max} \sim t^2$. Correspondingly, for a wave function in the momentum representation the momentum is restricted to the interval $|p| < p_{max} \sim t$. Outside of this region the wave function can be presented in terms of a Moshinsky-type function [W. van Dijk and Y. Nogami, Phys. Rev. Lett. **83**, (1999) 2867].
8. M. L. Chiofalo and M. P. Tosi, Phys. Lett. A **268**, (2000) 406.